

Fatigue Performance: Asphalt Binders versus Mixtures versus Full-Scale Pavements

Ghazi Al-Khateeb, Kevin Stuart, Walaa Mogawer and Nelson Gibson

Address for correspondence: Ghazi Al-Khateeb, Department of Civil Engineering, Jordan University of Science and Technology, P.O. Box 3030, Irbid 22110, Jordan: ggalkhateeb@just.edu.jo. Kevin Stuart is a Former Highway Research Engineer with the US Federal Highway Administration, Walaa Mogawer is Professor of Civil Engineering at the University of Massachusetts Dartmouth, and Nelson Gibson is a Highway Research Engineer with the US Federal Highway Administration.

Abstract

The Federal Highway Administration (FHWA) built 12 asphalt pavements in 1993 to validate Superpave tests and specifications used to measure the rutting and fatigue cracking performances of hot-mix asphalts and asphalt binders. Each pavement had four test sites. These sites were tested for either rutting or fatigue cracking using the FHWA's Accelerated Loading Facility (ALF). The main objective of the study documented in this paper was to compare the fatigue performance results from laboratory bending beam fatigue tests to the ALF fatigue cracking data obtained for these sites from lanes 1 through 4. The four lanes consisted of two asphalt pavement layer thicknesses (100 and 200 mm) and two asphalt binders (PG 58-34 and PG 64-22). Each lane was tested at three temperatures 10, 19, and 28 °C. Another objective of this study was to investigate the relationship between the asphalt binder parameter for intermediate temperature performance ($G^ \sin \delta$) and asphalt pavement fatigue life.*

Findings of this study showed that a relatively good correlation was obtained between the ALF pavement fatigue life and the asphalt mixture fatigue life from the strain-controlled bending beam fatigue tests. Comparison of the fatigue results at the three test temperatures showed rational trends with the longest fatigue life at 28 °C and the shortest fatigue life at 10 °C. Fatigue power models at these test temperatures were also obtained for asphalt mixtures produced using the two asphalt binders.

Acknowledgement

The authors would like to thank Scott Parobeck and Frank Davis for preparing the asphalt mixtures and fabricating the beam specimens for the bending beam fatigue tests, and Susan Needham for conducting the asphalt binder tests.

Disclaimer

The opinions, findings, and conclusions expressed in this paper are those of the authors only and not necessarily of Jordan University of Science and Technology nor of the Federal Highway Administration.

1.0 Introduction

Fatigue failure is known to occur when asphalt pavements undergo repeated loading in the intermediate temperature range from approximately 10°C to 30°C. Significant research has been conducted to understand fatigue cracking and to predict fatigue performance of asphalt pavements. Some researchers, (e.g., Monismith and Deacon, 1969; Van Dijk, 1975 and Kim *et al.*, 1997) characterized fatigue of asphalt mixtures using different theories. Other researchers investigated the factors affecting fatigue response performance. For example, Pell and Cooper, 1975 and Epps and Monismith, 1969 studied the influence of mixture variables on fatigue performance and properties. Raithby and Sterling, 1970; Bonnaure *et al.*, 1982 and Smith and Hesp, 2000 evaluated the effect of rest periods on fatigue performance, characteristics, and fatigue life of bituminous mixtures under repeated loading. Irwin and Gallaway, 1974 and Porter and Kennedy, 1975 referred to the influence of fatigue laboratory test methods on fatigue results for asphaltic concrete.

Several laboratory methods and various experimental techniques were cited in the literature to conduct fatigue testing and to characterize fatigue for asphalt paving mixtures. The majority of researchers, (e.g., Monismith and Deacon, 1969; Tayebali *et al.*, 1992, 1993, Carpenter *et al.*, 2003, and Al-Khateeb and Shenoy, 2004) used the bending beam fatigue test set up to conduct fatigue testing for asphalt mixtures. A few researchers including Rowe, 1993 and Kim *et al.*, 1990 used the trapezoidal configuration and the uniaxial configuration for cylindrical specimens, respectively, to test bituminous mixtures for fatigue.

Methods and procedures to analysis fatigue testing data varied from research group to another as cited in the literature. Definition of fatigue failure (or the number of load cycles to failure) and determination of the fatigue failure point in fatigue testing has been defined in various ways. Many researchers considered the reduction in initial stiffness in fatigue testing as a measure of fatigue failure. Others observed crack propagation to track fatigue failure and some others introduced dissipated energy concepts to define fatigue failure. Most of the time, the pinning of fatigue failure during a fatigue test was also correlated with the mode of loading. Nevertheless, Al-Khateeb and Shenoy, 2004 developed a fatigue failure criterion that is simple, fundamental, and independent of the mode of loading.

This paper documents part of a Federal Highway Administration (FHWA) research study that was performed to assist the highway community in validating Superpave performance-based tests, specifications, and prediction models for asphalt binders and mixtures. Twelve full-scale asphalt pavements were constructed in 1993 at the FHWA's Turner-Fairbank Highway Research Center in McLean, VA, and rutting as well as fatigue performance tests were conducted on these asphalt pavements until 2001 to validate tests for rutting and fatigue cracking. Each pavement had four sites that were tested by an Accelerated Loading Facility (ALF), which is a full-scale pavement-testing machine that applies one-half of a rear truck axle load. The pavements were tested using temperatures, loads, and loading distributions (wheel wander) that promoted either rutting or the formation of fatigue cracks in the asphalt pavement layer.

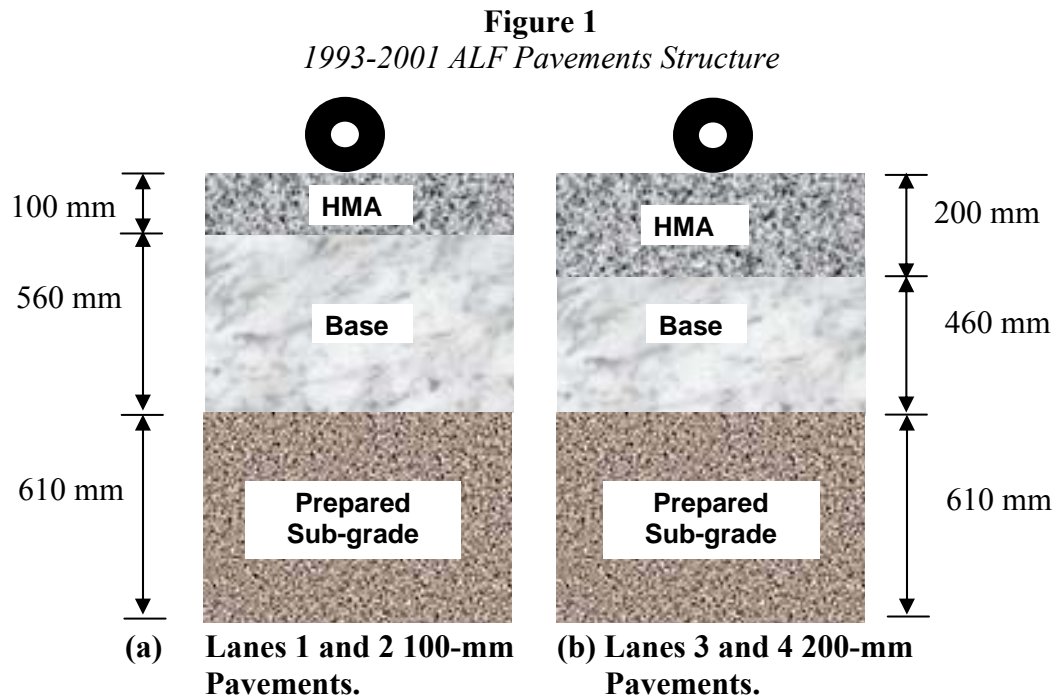
Lanes 1, 2, 3, and 4 were used to conduct the fatigue cracking study, while lanes 5 through 12 were primarily used to conduct the rutting study. The results of rutting studies were also presented elsewhere (Stuart *et al.*, 1999, 2001). The primary objectives of the fatigue cracking study were to validate the Superpave asphalt binder parameter for fatigue cracking, $G^* \sin \delta$, and to quantify the interacting effects of asphalt binder grade, asphalt pavement layer thickness, and pavement temperature on fatigue cracking performance. $G^* \sin \delta$ is the absolute value of the

complex shear modulus times the sine of the phase angle. Another objective of the fatigue study was to validate the strain-controlled bending beam fatigue test developed during the Strategic Highway Research Program.

2.0 ALF Asphalt Pavements

2.1 Pavement Structure and Materials

The asphalt pavement structure in lanes 1 through 4 consisted of a single hot-mix asphalt (HMA) on top of an unbound crushed aggregate base and prepared subgrade (Figure 1). The thickness of the asphalt pavement layer was 100 millimeters (mm) in lanes 1 and 2, and 200 mm



in lanes 3 and 4. The thickness of the unbound crushed aggregate base layer was 560 mm in lanes 1 and 2, and 460 mm in lanes 3 and 4. The prepared subgrade had a thickness of 610 mm in all lanes.

The asphalt mixtures in lanes 1 through 4 consisted of two asphalt binders and a single aggregate gradation. Both binders were from Venezuela's Lagoven base stock. Table 1 shows the Superpave performance grades (PGs) of the original asphalt binders (PG 58-34 and PG 64-22) and the continuous PG after the rolling thin-film oven (RTFO) test and after the pressure aging vessel (PAV) test. A diabase aggregate with a 19.0-mm nominal maximum aggregate size was used for the HMA in lanes 1 through 4 with the gradation shown in Figure 2. (Diabase is a dark-gray to black, fine-textured igneous rock composed mainly of feldspar and pyroxene and used for monuments and as crushed stone.) The continuous intermediate temperature PG is defined as the temperature at a $G^* \sin \delta$ value of 5000 kPa and a frequency of 10.0 rad/s. Each mixture should be highly resistant to fatigue cracking at temperatures above its intermediate temperature PG.

Table 1
Asphalt Binders Used in the ALF Pavements

(a) Asphalt Binders by Lane

Lane	1	2	3	4
PG	58-34	64-22	58-34	64-22
Continuous High PG*	59	68	59	68
Continuous High PG* after RTFO Test	59	70	59	70
Asphalt Binder Content, %	4.7	4.8	4.8	4.9

* Temperature at which PG requirements met.

(b) Superpave PGs of the Asphalt Binders

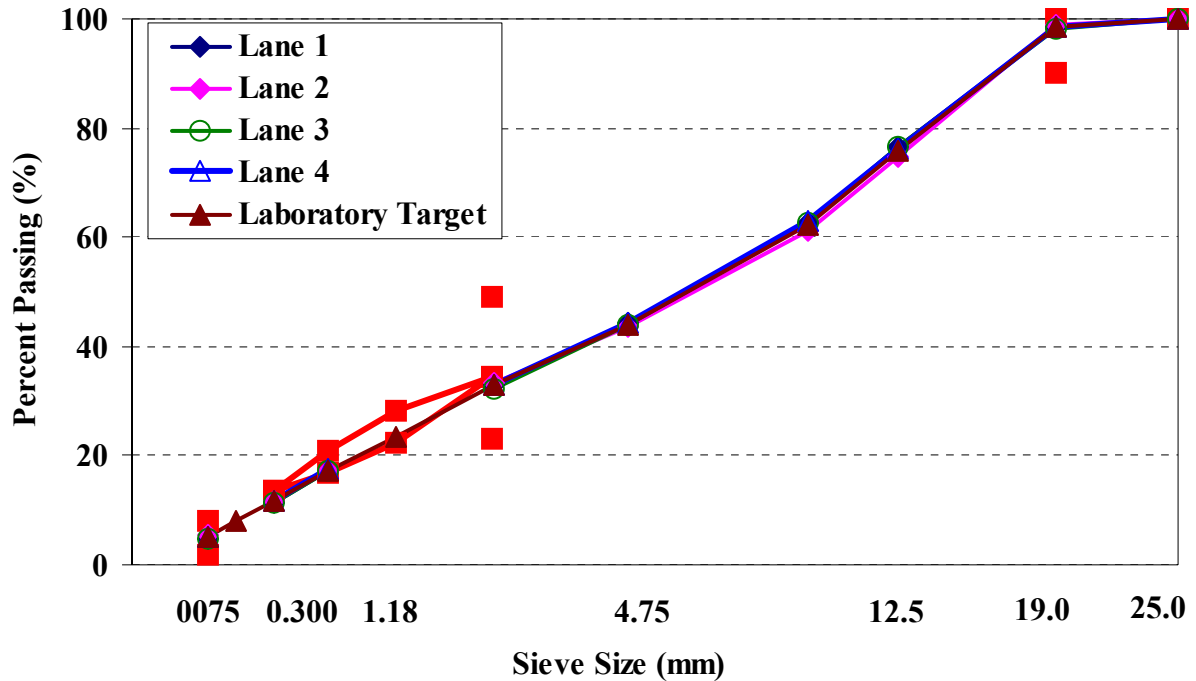
	PG 58-34	PG 64-22
Original Asphalt Binder		
Temperature at a $G^*/\sin\delta$ of 1.00 kPa and 10 rad/s, °C	59	68
RTFO Residue		
Temperature at a $G^*/\sin\delta$ of 2.20 kPa and 10 rad/s, °C (Continuous High Temperature PG)	59	70
RTFO*/PAV** Residue		
Temperature at a $G^*\sin\delta$ of 5000 kPa and 10 rad/s, °C (Continuous Intermediate Temperature PG)	9	17
Temperature based on a Creep Stiffness (S) of 300 MPa and 60 s, °C	-37	-30
Temperature based on an m-value of 0.30 and 60 s, °C	-35	-27

* RTFO = Rolling Thin-Film Oven; ** PAV = Pressure Aging Vessel.

Table 2
ALF Testing for Fatigue Cracking Resistance

Lane	Asphalt Pavement Layer Thickness (mm)	Pavement Test Temperature and Year of Test		
		28°C	19°C	10°C
1	100	1994 to 1995	1997 to 1998	1997 to 1998
2	100	1994 to 1995	1997 to 1998	1997 to 1998
3	200	1995 to 1996	1996 to 1997	1999 to 2000
4	200	1995 to 1996	1996 to 1997	2000 to 2001

Figure 2
Aggregate Gradation for Each Lane



2.2 Pavement Testing Sequence

The pavements were tested during October through April when the weather was cool in order to obtain and maintain the required pavement test temperature. The pavements could be heated using infrared heat lamps, but the ALF system did not have the capability of cooling them. Table 2 shows the fatigue testing schedule. Fatigue testing started when the pavements were 1-year old.

2.3 ALF Pavement Testing

ALF contains a moving wheel assembly that applies one-half of a rear truck axle load. The ALF machines have long frames of 29 m (95 ft) length with rails to direct rolling wheels. Each ALF machine was capable of applying an average of 35,000 wheel passes per week using a half-axle load ranging from 33 to 84 kN (7,500 to 19,000 lbf). The load was applied in one direction to a 14 m (45 ft) length of pavement at a speed of 18.5 kph (11.6 mph). The machines could allow testing with conventional dual truck tires or wide-based “super-single” tires and simulation of the real-world lateral distribution of truck loadings using programmed transverse wheel wander. To simulate highway traffic, the ALF applies loading on the pavement in one direction only, and the loads can also be distributed from side to side to simulate wheel wander.

The ALF was operated using the following protocols:

- Super single tire.
- Load of 53.0 kN, and tire pressure of 690 kPa.

- Speed of 18.5 kph.
- Full wheel wander with a width of 1070 mm.
- Wheelpath length of 10.0 m.
- Controlled pavement temperatures of 10, 19, and 28°C.

A minimum of seven distress surveys was performed on each pavement during trafficking. The surveys included measuring transverse and longitudinal profiles and mapping surface cracks. The pavements were cored and trenched after testing. The continuous intermediate temperature PGs of the asphalt binders recovered from the cores are given in Table 3. Age hardening did not affect these PGs as shown in the table. Thus, it was assumed that all of the fatigue beams could be aged using the same protocol. The high- temperature properties of the recovered asphalt binders did show that the asphalt binders aged with time.

Table 3
Continuous Intermediate Temperature PGs of the Asphalt Binders

PG after RTFO and PAV aging	PGs of Pavement Cores					
	1995	1996	1997	1998	1999	2000
9	9	9	10	10	9	10
17	19	16	18	20	18	15

ALF pavement fatigue life was based on the number of wheel passes when the first crack appeared on the surface of the pavement, and on the number of wheel passes at cumulative crack lengths of 50 m and 100 m. The percent area cracked was also measured. However, this measurement provided the same relative fatigue lives as cumulative crack length. Thus, they are not included in this paper.

2.5 Mechanistic Analysis

A mechanistic analysis was conducted using the WinJULEA program to estimate the tensile strains at the bottom of the asphalt layer for each pavement. The inputs needed for each layer were the thickness, modulus, and Poisson's ratio. The moduli of the crushed aggregate base and subgrade were backcalculated from the data provided by falling weight deflectometer (FWD) tests, which were conducted on the asphalt pavement layer after the pavements were constructed. The program used to do the backcalculations was BOUSDEF. These moduli are given in Table 4(a). Table 4(b) provides the moduli of the asphalt mixtures at the three temperatures (10, 19, and 28°C). These moduli were measured using the indirect tensile test at these three pavement test temperatures. Typical Poisson's ratios were used as inputs to the WinJULEA program: 0.35 for the asphalt layer, 0.40 for the crushed aggregate base layer, and 0.45 for the subgrade layer. Other inputs were the load of 53 kN, the radius of the loading area, which was 159 mm, and the location where the tensile stresses and strains needed to be determined, which was at the bottom of the asphalt layer. Table 5 provides the tensile strains obtained from the WinJULEA program.

3.0 Laboratory Bending Beam Fatigue Testing

3.1 Sample Preparation

The asphalt binders were heated to 163°C and mixed with heated aggregates in proportion to achieve a binder content of 4.8 percent by the total mass of the mixture.

The loose asphalt mixtures were short-term oven aged at 135°C for 2 hours according to the AASHTO provisional practice PP2-00 (2000). This degree of aging was found to match the average amount of aging in the pavements prior to the first pavement test. The short-term aged asphalt mixtures were compacted using a Slab-Pak™ linear kneading compactor into 180 × 500 × 50-mm slabs. Fatigue beams were then cut from the slabs. The target air-void level for the beams was 7.0 ± 0.5 percent. The air-void range of the pavements was 7.0 ± 1.2 percent.

Table 4
Moduli of the Different Pavement Materials

(a) Moduli of the Unbound Aggregate and the Prepared Subgrade

Lane	Thickness (mm)		Sites	Modulus From Elastic Layer Analysis (MPa)	
	Asphalt Pavement Layer	Crushed Aggregate Base		Crushed Aggregate Base	Prepared Subgrade
1	100	560	1 and 2	340	60
			3 and 4	302	41
2	100	560	1 and 2	228	56
			3 and 4	202	45
3	200	460	1 and 2	340	38
			3 and 4	302	29
4	200	460	1 and 2	339	41
			3 and 4	483	28

(b) Moduli of the Asphalt Mixtures from the Indirect Tensile Test

Lanes	PG after RTFO and PAV Aging*	Tensile Modulus (MPa)		
		10°C	19°C	28°C
1 and 3	9	4050	1975	826
2 and 4	17	7466	3452	1765

*The performance grade of the asphalt binders used for lanes 1 and 3 and 2 and 4 after being aged in the RTFO = Rolling Thin-Film Oven and PAV = Pressure Aging Vessel.

3.2 Testing Procedure

Bending beam fatigue tests were performed in accordance with the AASHTO provisional test method TP8-94 (21). The tests were conducted in the strain-controlled mode of loading. In this test, a vertical sinusoidal displacement is applied to a beam at a frequency of 10 Hz with no rest periods. The required vertical displacement is calculated from the desired peak strain and beam geometry according to Equation (1) shown below. Four strain levels were used in the fatigue testing: 300, 600, 900, and 1200 $\mu\epsilon$.

$$\epsilon_t = \frac{12d \times h}{3l^2 - 4a^2} \quad (1)$$

Table 5
Tensile Strains at the Bottom of the Asphalt Layer for All Pavements

Lane	Asphalt Pavement Layer Thickness (mm)	Pavement Test Temperature ($^{\circ}\text{C}$)	WinJULEA Tensile Strain at the Bottom of the Asphalt Layer ($\mu\epsilon$)
1	100	28	476
		19	390
		10	294
2	100	28	431
		19	332
		10	224
3	200	28	279
		19	208
		10	146
4	200	28	188
		19	142
		10	95

where:

ϵ_t = maximum tensile strain;

d = maximum vertical deformation at the center of the beam;

h = average specimen height;

l = length of beam between outside clamps; and

a = space between inside clamps = $l/3$.

Two concentrated and symmetrical loads are applied on the fatigue beam specimen, as shown in Figure 3. The beam specimen is forced back to its original position at the end of each load pulse. It is subjected to 4-point bending. Free rotation and horizontal translation are allowed at all load and reaction points.

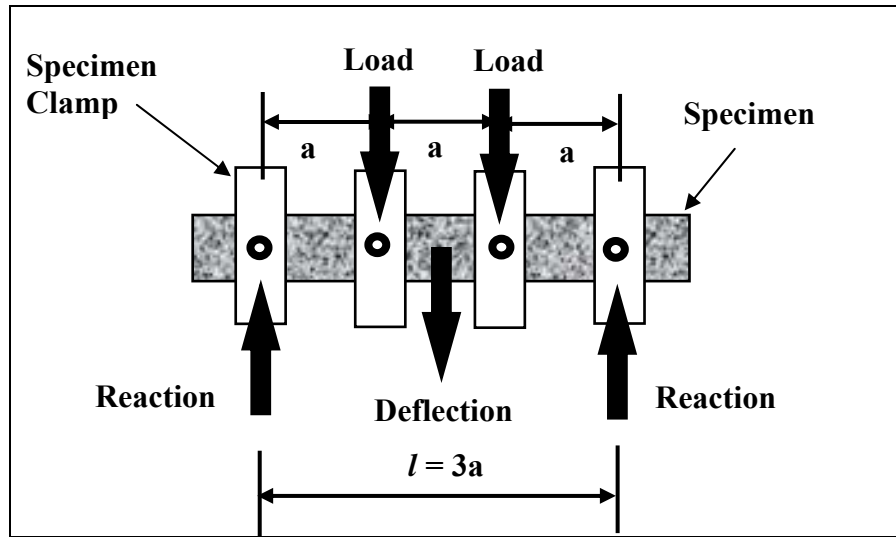
The data acquisition software (TestStar™) recorded the load and the deformation of the specimen per cycle of loading. The peak tensile stress required to obtain the desired peak strain for each loading cycle was calculated using Equation (2) below:

$$\sigma_t = \frac{lP}{bh^2} \tag{2}$$

where:

- σ_t = maximum tensile stress;
- P = load applied by actuator; and
- b = average specimen width.

Figure 3
Bending Beam Fatigue Test Schematic Diagram



The flexural modulus or stiffness (S) was then computed by dividing the peak stress by the applied peak strain as shown in Equation (3).

$$S = \frac{\sigma_t}{\epsilon_t} \tag{3}$$

4.0 Bending Beam Fatigue Test Results

In the fatigue test, the modulus (stiffness) of the beam specimen decreases with loading. Since fatigue tests are conducted in the strain-controlled mode (the applied strain is constant), the resulting stress in the specimen decreases with time (or loading). In this study, the most common and widely used fatigue failure method adopted by the AASHTO provisional test method TP8-94 is suggested to define fatigue failure, which is the point at which 50-percent reduction in initial stiffness occurs. However, in this study, a 40-percent reduction was used because the use of 50 percent would require either extremely long tests or a high number of extrapolations. Thus, a 40-percent reduction in the flexural modulus appeared to be optimal.

At a given temperature, each applied strain provides a different number of cycles to failure. The relationship between the applied strain and fatigue life is obtained at each temperature. This relationship is typically used to estimate the fatigue life of an asphalt mixture used in a pavement

design. The pavement design provides a tensile strain at the bottom of the asphalt layer using the mechanistic analysis of the pavement. This strain is then used as an input to the relationship to determine the fatigue life. In this study, the strains obtained from the WinJULEA program were used as the inputs.

Normally already developed laboratory-to-field shift factors are used to predict the number of equivalent single-axle loads at failure from the bending beam fatigue test results, and to account for differences between the laboratory and the field, such as boundary conditions. Nevertheless, shift factors were not used in this study. The fatigue lives from the bending beam fatigue tests were directly compared to the fatigue lives of the ALF pavements.

Table 6 provides the fatigue coefficients K_1 and K_2 obtained from the developed power model for the relationship between the applied tensile strain and the number of load cycles to failure. The average numbers of cycles at failure based on a 40-percent reduction in the flexural modulus are shown in Table 7. The data using 50- and 30-percent reductions are included as supplemental information. Table 7 also provides the strains actually applied during the bending beam fatigue test. These strains are slightly different from the nominal or desired strain. The relationship between the applied strain and the number of load cycles to failure was developed for the two asphalt mixtures at the three test temperatures (10, 19, and 28°C) using the results tabulated in Table 7 as shown in Figure 4. The developed relationship is a power model of the form shown in Equation (4) below.

$$N_f = K_1(\varepsilon)^{K_2} \quad (4)$$

where:

- N_f = number of load cycles to fatigue failure,
- K_1 and K_2 = regression coefficients, and
- ε = applied tensile strain in microstrains.

As noted, the intercept coefficient, K_1 and the power coefficient, K_2 obtained for the two asphalt mixtures at the three test temperatures are in Table 6.

Table 6
*Fatigue Coefficients K_1 , and K_2 for PG 58-34 and
PG 64-22 Asphalt Mixtures at Test Temperatures of 10, 19, and 28 °C*

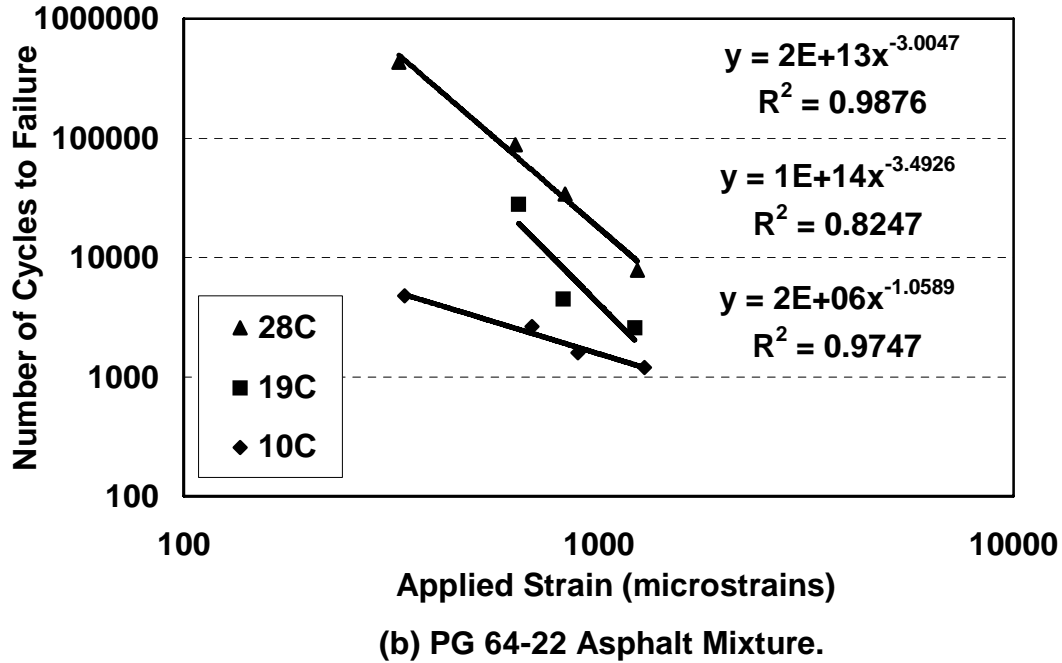
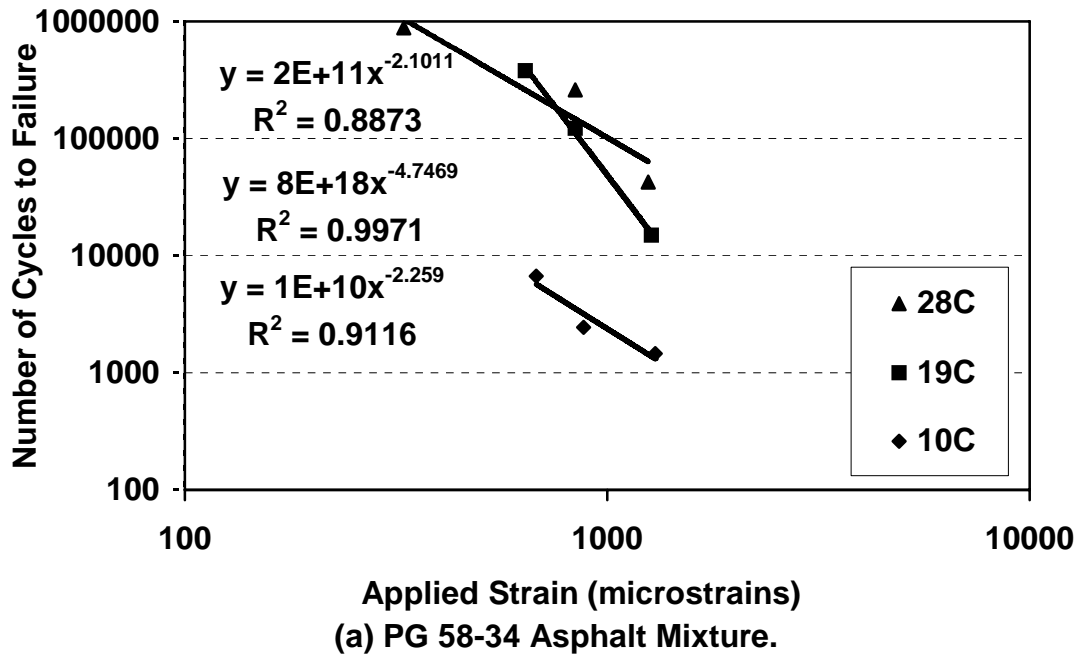
Asphalt Mixture	Test Temperature (°C)	K_1	K_2	R^2
PG 58-34	28	2×10^{11}	-2.1011	0.887
	19	8×10^{18}	-4.7469	0.997
	10	1×10^{10}	-2.2590	0.912
PG 64-22	28	2×10^{13}	-3.0047	0.988
	19	1×10^{14}	-3.4926	0.825
	10	2×10^6	-1.0589	0.975

Table 7
*Number of Load Cycles to Failure from the Bending Beam Fatigue Test
 and the Actual Applied Strains*

Desired Strain ($\mu\epsilon$)	PG 58-34			PG 64-22		
	28°C	19°C	10°C	28°C	19°C	10°C
Based on a 50-percent Reduction in Flexural Modulus						
300	12,500,000	ND*	ND	5,000,000	ND	8,690
600	ND	4,000,000	13,400	490,000	140,000	4,170
900	1,980,000	970,000	3,770	160,000	10,100	2,400
1200	186,000	48,000	2,260	18,200	5,000	2,090
Based on a 40-percent Reduction in Flexural Modulus						
300	880,000	ND	ND	430,000	ND	4,740
600	ND	380,000	6,660	88,000	28,000	2,620
900	261,000	123,000	2,440	34,000	4,470	1,590
1200	42,500	15,000	1,460	7,800	2,560	1,200
Based on a 30-percent Reduction in Flexural Modulus						
300	98,200	ND	ND	56,800	ND	2,870
600	ND	55,000	3,740	21,100	9,000	1,800
900	48,300	25,200	1,690	10,900	2,410	1,130
1200	12,400	5,800	1,020	3,950	1,460	760
Actual Applied Strain for Each Desired Strain						
300	330	330	330	330	330	340
600	640	640	680	630	640	690
900	840	840	880	830	820	890
1200	1250	1270	1300	1240	1220	1290

* ND = No data.

Figure 4
Beam Fatigue Cycles to Failure vs Applied Strain Level



5.0 Fatigue Performance Comparisons

5.1 ALF Pavement Performance vs. Bending Beam Fatigue Test Results

The fatigue lives of the asphalt mixtures based on the bending beam fatigue test and ALF pavement performance are shown in Table 8. Table 8(a) groups the pavement data by lane. This shows the effect of test temperature on fatigue life while Table 8(b) groups the data to show the effect of the asphalt binder parameter, $G^* \sin \delta$, on fatigue life. $G^* \sin \delta$ was obtained from the dynamic shear rheometer (DSR) using the ALF-associated loading frequency of 2.25 rad/s. The asphalt binders were aged using the rolling thin-film oven (RTFO) and pressure-aging vessel (PAV). The bending beam fatigue test results and the fatigue performance of the ALF pavements agree with each other particularly well at the test temperature of 28°C. Figure 5 shows the relatively high correlation between the two as the R^2 values were 0.63 and 0.99 for all test temperatures together and at the test temperature of 28°C, respectively.

For a given asphalt mixture, the best laboratory fatigue performance was obtained at 28°C and the worse performance was obtained at 10°C as shown in Figure 4. These findings are to be expected as asphalt mixtures tend to become stiffer at lower intermediate temperatures and therefore their resistance to fatigue cracking becomes lower. A similar trend was obtained for the fatigue performance of the ALF pavements as the correlation between the two was found to be relatively high at the three test temperatures.

For ALF lanes constructed using the same asphalt mixture (lanes 1 and 3 or lanes 2 and 4), the asphalt layer thickness did impact the fatigue performance at the ALF sites. For instance, lane 3 with the PG 58-34 asphalt mixture performed better than lane 1 with the same asphalt mixture. Also lane 4 with the PG 64-22 asphalt mixture had better fatigue cracking resistance than lane 2 with the same asphalt mixture. This finding applied to all test temperatures (10, 19, and 28°C). Thus, regardless of the test temperature, field fatigue performance for thick asphalt pavements was found to be better than that for thin asphalt pavements.

5.2 ALF Pavement Performance vs. Asphalt Binder $G^* \sin \delta$

Figure 6(a) shows the relationship between the ALF wheel passes to initial cracking and the asphalt binder $G^* \sin \delta$ for the pavements with a HMA layer thickness of 100 mm. Figure 6(b) shows similar relationship for the pavements with a HMA layer thickness of 200 mm. As shown in these figures, a high coefficient of determination (R^2) between the ALF fatigue parameter and the asphalt binder parameter ($G^* \sin \delta$) was obtained particularly for the 100-mm thick pavements. The R^2 values obtained were 0.80 and 0.40 for the 100-mm and 200-mm thick pavements, respectively. It has been noted that one or sometimes two outlier(s) were excluded from the analysis due to the fact that this or these data point(s) either corresponded to pavement section(s) that cracked and rutted very quickly because of a local weakness in the crushed aggregate base layer or were obtained using extrapolations.

The trend shown in Figure 6(a) indicates that at lower values of $G^* \sin \delta$, the number of the ALF wheel passes to initial cracking tends to be higher due to the fact that lower $G^* \sin \delta$ values leads to increased flexibility and therefore longer fatigue life. This indicates a strain-controlled response and agrees with the asphalt binder Superpave specifications.

Table 8(a)
ALF Wheel Passes to Failure vs. Bending Beam Fatigue Test Results Grouped By Lane

Pavement Variable			ALF Wheel Passes at Three Failure Modes			Beam Fatigue Test
Lane	Thickness (mm)	Test Temp. (°C)	Initial Crack	Crack Length of 50 m	Crack Length of 100 m	Cycles to Failure*
1	100	28	100,000	200,000	220,000	40,400
		19	<1,000	4,000	8,000	86,200
		10	14,000	25,000	43,000	10,200
2	100	28	50,000	160,000	180,000	20,500
		19	10,000	39,000	75,000	24,300
		10	20,000	50,000	85,000	4,620
3	200	28	300,000	320,000	350,000	139,000
		19	25,000	75,000	160,000	2,800,000
		10	250,000	>400,000	>400,000	78,600
4	200	28	350,000	460,000	530,000	240,000
		19	150,000	410,000	540,000	1,010,000
		10	220,000	>400,000	>400,000	13,000

* Fatigue failure in this case is based on 40-percent reduction in initial stiffness.

The relationship in Figure 6(b), on the other hand, provides a lower R^2 value (0.40) and similar trend to that for the 100-mm thick pavements. In other words, as the $G^* \sin \delta$ value gets higher, the number of the ALF wheel passes to initial cracking becomes lower due to the increased stiffness of the asphalt mixture and thus reduced flexibility.

The relationship between the ALF wheel passes to a cumulative crack length of 50 m and $G^* \sin \delta$ for the 100-mm thick asphalt pavements demonstrated in Figure 7(a) having a R^2 value of 0.80 was similar to that shown in Figure 6(a) when initial cracking was considered. However, an opposite trend to that shown in Figure 6(b) was obtained between the ALF wheel passes to a cumulative crack length of 50 m and $G^* \sin \delta$ for the 200-mm thick asphalt pavements as illustrated in Figure 7(b) with a R^2 value of 0.66. Although higher $G^* \sin \delta$ values results in reduced flexibility, but thicker asphalt layers compensates for the increased stiffness that becomes an advantageous property for fatigue resistance for pavements with thicker asphalt layers over pavements with thinner asphalt layers due to the lower strain levels obtained. In this case, a high $G^* \sin \delta$ value is preferred, and a value such as 2000 kPa should be used as a minimum pass/fail criterion. Below 2000 kPa, there is a wide range of pavement performances which have weak relationship with $G^* \sin \delta$.

Table 8(b)
ALF Wheel Passes to Failure vs. Bending Beam Fatigue Test Results Grouped By Temperature plus Asphalt Binder $G^ \sin \delta$ Data*

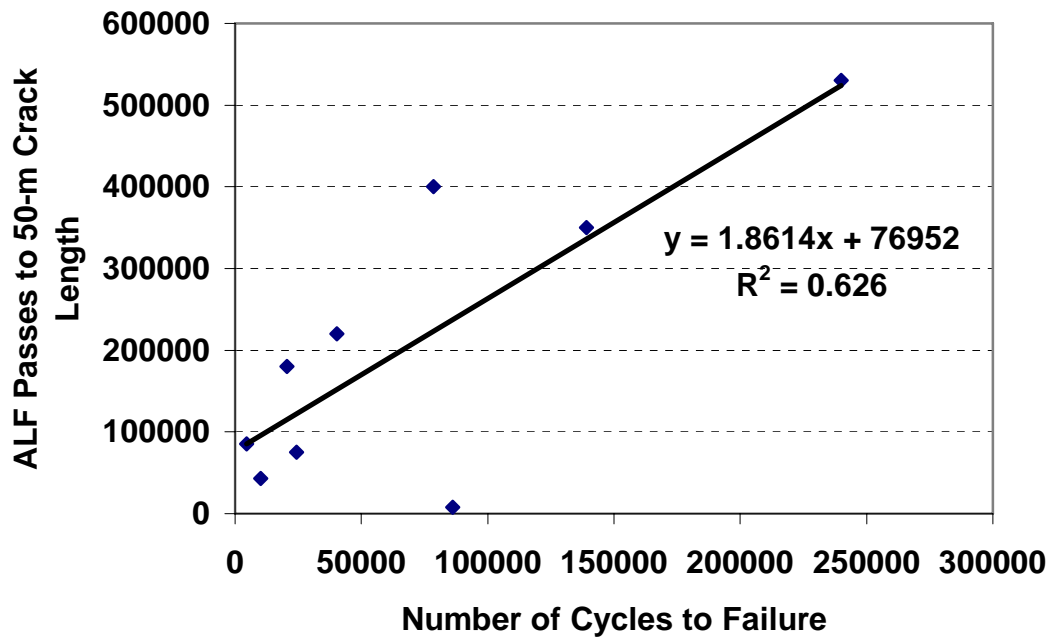
Pavement Variable				ALF Wheel Passes at Three Failure Modes			Beam Fatigue Test
Lane	Thickness (mm)	Test Temp. (°C)	$G^* \sin \delta$ of the Asphalt Binder (kPa)	Initial Crack	Crack Length of 50 m	Crack Length of 100 m	Cycles to Failure
1	100	28	213	100,000	200,000	220,000	40,400
2			680	50,000	160,000	180,000	20,500
3	200	28	213	300,000	320,000	350,000	139,000
4			680	350,000	460,000	530,000	240,000
1	100	19	720	<1,000	4,000	8,000	86,200
2			2150	10,000	39,000	75,000	24,300
3	200	19	720	25,000	75,000	160,000	2,800,000
4			2150	150,000	410,000	540,000	1,010,000
1	100	10	2443	14,000	25,000	43,000	10,200
2			6821	20,000	50,000	85,000	4,620
3	200	10	2443	250,000	>400,000	>400,000	78,600
4			6821	220,000	>400,000	>400,000	13,000

The proportional relationship between the ALF wheel passes to a cumulative crack length of 50 m and $G^* \sin \delta$ for the 200-mm thick asphalt pavements suggests that the stress-controlled parameter, $G^* \sin \delta$, should be used for evaluating the fatigue performance for the thick pavements. Figure 8 shows the relationship using $G^* \sin \delta$. The R^2 value of this relationship is 0.66. It can be concluded that for the thick pavements, the use of an asphalt binder with a $G^* \sin \delta$ value below approximately 5000 kPa will provide a greater chance of having poorer fatigue performance. This proves that the response is stress-controlled at all temperatures.

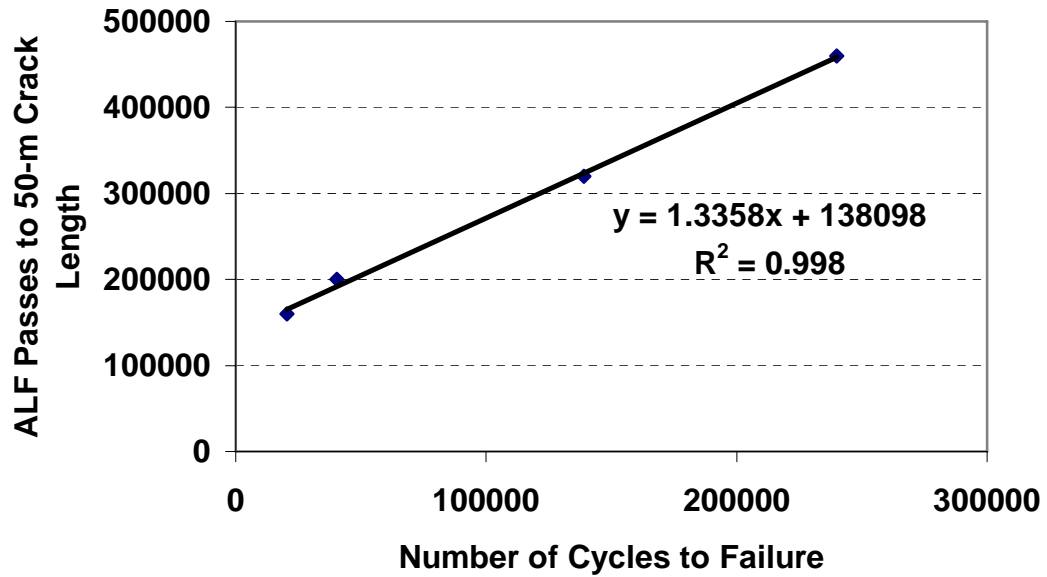
For thick asphalt pavements, it cannot be concluded that above a certain strain level, performance will be strain-controlled, and below it, performance will be stress-controlled. For example, thick pavements with strain levels of 422 and 429 microstrains have widely different number of ALF wheel passes to fatigue failure. This means that the fatigue performance of the thicker pavements was not a function of the strain level alone.

Figure 5

ALF Wheel Passes to 50-m Crack Length vs. Beam Fatigue Cycles to Failure



(a) Not Showing Temperatures Separately.



(b) At Test Temperature of 28C.

Figure 6
ALF Wheel Passes to Initial Cracking vs Asphalt Binder $G^\sin\delta$*

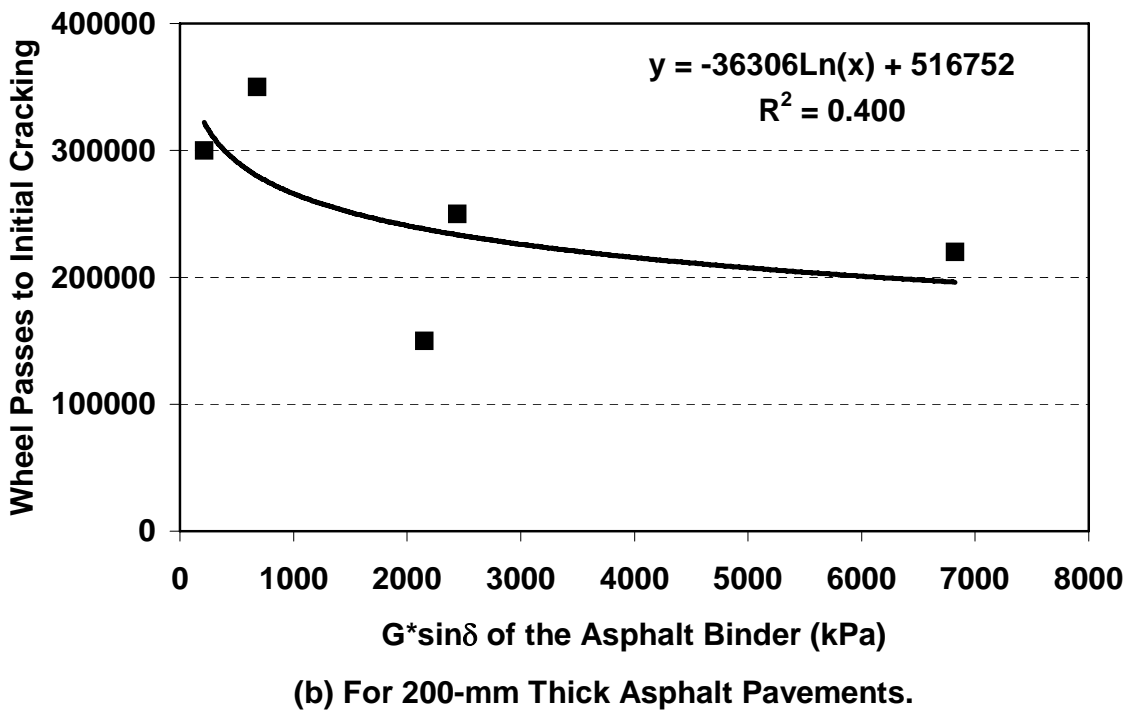
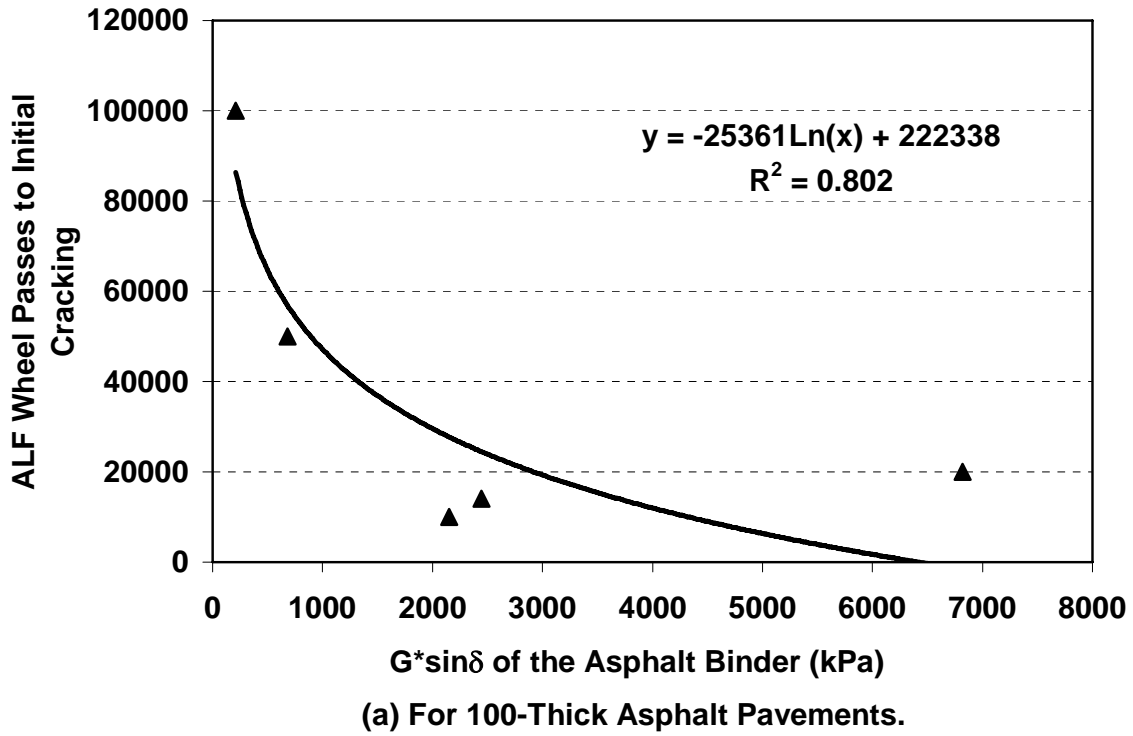
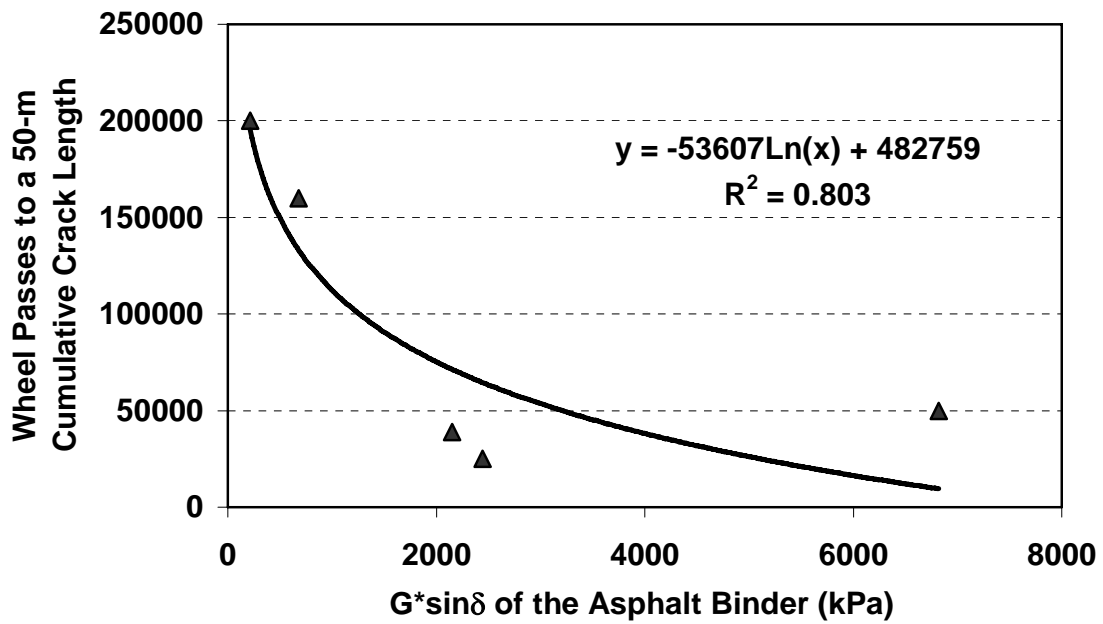
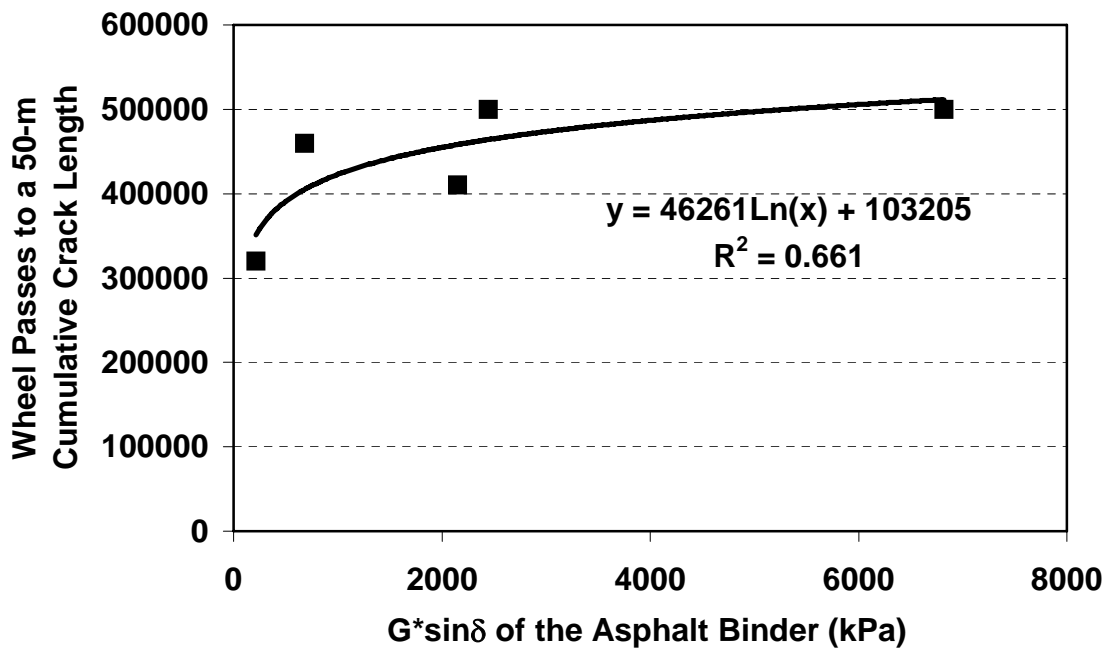


Figure 7

ALF Wheel Passes to 50-m Cumulative Crack Length vs. Asphalt Binder $G^\sin\delta$*

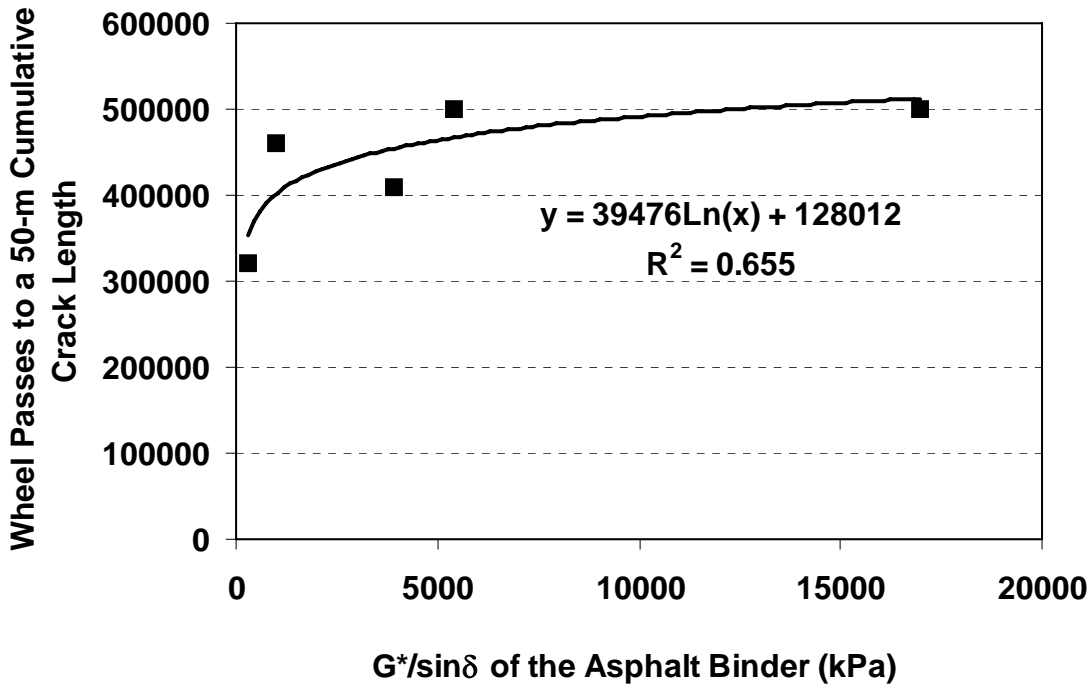


(a) For 100-mm Thick Asphalt Pavements.



(b) For 200-mm Thick Asphalt Pavements.

Figure 8
ALF Wheel Passes to 50-m Cumulative Crack Length vs. Asphalt Binder $G^/\sin\delta$ for the 200-mm Thick Pavements*



6.0 Conclusions

Based on the results of this study, a number of conclusions may be drawn. After trying several different forms including exponential, logarithmic, and linear, it was found that the relationship between the applied strain and the number of fatigue load cycles to failure was best represented by a power model of the form $N_f = K_1(\varepsilon)^{K_2}$.

For a given asphalt mixture, the best laboratory fatigue performance was obtained at 28°C and the worse performance was obtained at 10°C. The bending beam fatigue test results and the fatigue performance of the ALF pavements agreed with each other particularly well at the test temperature of 28°C although a relatively high correlation was also obtained for all test temperatures together..

Increasing the asphalt layer thickness improved the fatigue performance at the ALF sites for lanes constructed using the same asphalt mixture. A good coefficient of determination was obtained for the inverse relationship between the ALF wheel passes to initial cracking and the asphalt binder parameter ($G^* \sin\delta$) particularly for the thinner 100-mm thick pavements. As the $G^* \sin\delta$ value decreased, the number of the ALF wheel passes to initial cracking became higher due to the fact that lower $G^* \sin\delta$ values resulted in increased flexibility and therefore longer fatigue life.

A similar relationship was also obtained between the ALF wheel passes to a cumulative crack length of 50 m and $G^* \sin\delta$ for the 100-mm thick asphalt pavements but a direct

relationship was obtained between the ALF wheel passes to a cumulative crack length of 50 m and $G^* \sin \delta$ for the 200-mm thick asphalt pavements. This suggests that the stress-controlled parameter, $G^* / \sin \delta$, should be used for evaluating the fatigue performance for the thick pavements. It could be inferred that for the thick pavements, the use of an asphalt binder with a $G^* / \sin \delta$ value below approximately 5000 kPa would be more likely to exhibit poorer fatigue performance.

References

- American Association of State Highway and Transportation Officials (AASHTO) (2002) Method for determining the fatigue life of compacted hot-mix asphalt (HMA) subjected to repeated flexural bending. *AASHTO Provisional Standards*, TP8-94, Washington, D.C.
- American Association of State Highway and Transportation Officials (AASHTO) (2000) Standard practice for mixture conditioning of hot-mix asphalt (HMA). *AASHTO Provisional Standards*, PP2-00, Washington, D.C.
- Al-Khateeb, G.G. and A. Shenoy (2004) A distinctive fatigue failure criterion. *Journal of the Association of Asphalt Paving Technologists*, 62: 344-384.
- Bonnaure, F.P., A.H.J.J. Huibers, and A. Boonders (1982) A laboratory investigation of the influence of rest periods on the fatigue characteristics of bituminous mixes. *Journal of the Association of Asphalt Paving Technologists*, 51: 104-126.
- Carpenter, S.H., K.A. Ghuzlan and S. Shen (2003) A fatigue endurance limit for highway and airport pavements. *Transportation Research Record*, 1832: 131-138.
- Epps, J.A. and C.L. Monismith (1969) Influence of mixture variables on the flexural fatigue properties of asphalt concrete. *Journal of the Association of Asphalt Paving Technologists*, 38: 423-464.
- Irwin, L.H. and B.M. Gallaway (1974) Influence of laboratory test method on fatigue results for asphaltic concrete. *Fatigue and Dynamic Testing of Bituminous Mixtures*, ASTM Special Technical Paper 561: 12-46.
- Kim, Y.R., H.J. Lee, and D.N. Little (1997) Fatigue characterization of asphalt concrete using viscoelasticity and continuum damage theory. *Journal of the Association of Asphalt Paving Technologists*, 66: 520-569.
- Monismith, C.L. and J.A. Deacon (1969) Fatigue of asphalt paving mixtures. *Journal of Transportation Engineering*, 95(2): 317-345.
- Pell, P.S. and K.E. Cooper (1975) The effect of testing and mix variables on the fatigue performance of bituminous materials. *Journal of the Association of Asphalt Paving Technologists*, 44:1-37.
- Porter, B.W. and T.W. Kennedy (1975) Comparison of fatigue test methods for asphalt materials. *Research Report 183-4, Project 3-9-72-183*, Center for Highway Research, University of Texas at Austin, April 1975.
- Raithby, K.D. and A.B. Sterling (1970) The effect of rest periods on the fatigue performance of a hot-rolled asphalt under repeated loading. *Journal of the Association of Asphalt Paving Technologists*, 39: 134-152.
- Rowe, G.M. (1993) Performance of asphalt mixtures in the trapezoidal fatigue test. *Journal of the Association of Asphalt Paving Technologists*, 62: 344-384.

- Smith, B.J. and S.A.M. Hesp (2000) Crack pinning in asphalt mastic and concrete: effect of rest periods and polymer modifiers on the fatigue life. *Proceedings of 2nd Eurasphalt & Eurobitume Congress, Barcelona, Spain*, II: 539-546.
- Stuart, K.D., W.S. Mogawer, and P. Romero (1999) Validation of asphalt binder and mixture tests that measure rutting susceptibility using the accelerated loading facility. *Publication No. FHWA-RD-99-204, Federal Highway Administration, McLean, VA.*
- Stuart, K.D., W.S. Mogawer, and P. Romero (2001) Validation of the superpave asphalt binder fatigue cracking parameter using the FHWA's accelerated loading. *Publication No. FHWA-RD-01-093, Federal Highway Administration, McLean, VA.*
- Tayebali, A.A., J.A. Deacon, J.S. Coplantz, and C.L. Monismith (1993) Modeling fatigue response of asphalt-aggregate mixes (1993). *Journal of the Association of Asphalt Paving Technologists*, 62: 385-421.
- Tayebali, A.A., G.M. Rowe, and J.B. Sousa (1992) Fatigue response of asphalt-aggregate mixtures. *Journal of the Association of Asphalt Paving Technologists*, 61: 333-360.
- Van Dijk, W. (1975) Practical fatigue characterization of bituminous mixes. *Journal of the Association of Asphalt Paving Technologists*, 44: 38-72.